Chapter 4. Velocity Estimation for Diffracting Earth Models

We first turn our attention to the more general case of velocity estimation in which the subsurface reflectors may now assume non-zero dip and curvature. The subsurface reflector geometry will retain its property of being two-dimensional, and the velocity will remain a function of depth only (actually, we require only that it vary slowly enough in the x-direction so that it remains essentially constant over the distance between the near and far offsets).

An additional generalization to a medium with strong lateral velocity variations will require migration of not only the upcoming wave, but also of the downgoing wave. The generalized wave stack is introduced which, along with wave equation migration of the upcoming wave field, constitutes a complete migration procedure.

Dipping Layers in Slant Frames

As a preliminary to general diffracting earth models, we investigate the effects of dipping layers on velocity estimation in slant frames.

Figure 4.1 shows a ray path diagram for the slant frame geometry and a reflector with dip, ϕ . This figure should be compared to Figure 2.8, which describes the geometry for a horizontal reflector.

We find, with the help of the figure, that

$$\frac{t'}{t'_0} = \cos(\theta + \phi) \tag{4.1}$$

which reduces to equation (2.9a) for zero dip. The time parameter, t'_0 , is still the zero-offset, two-way shot to geophone time, but is

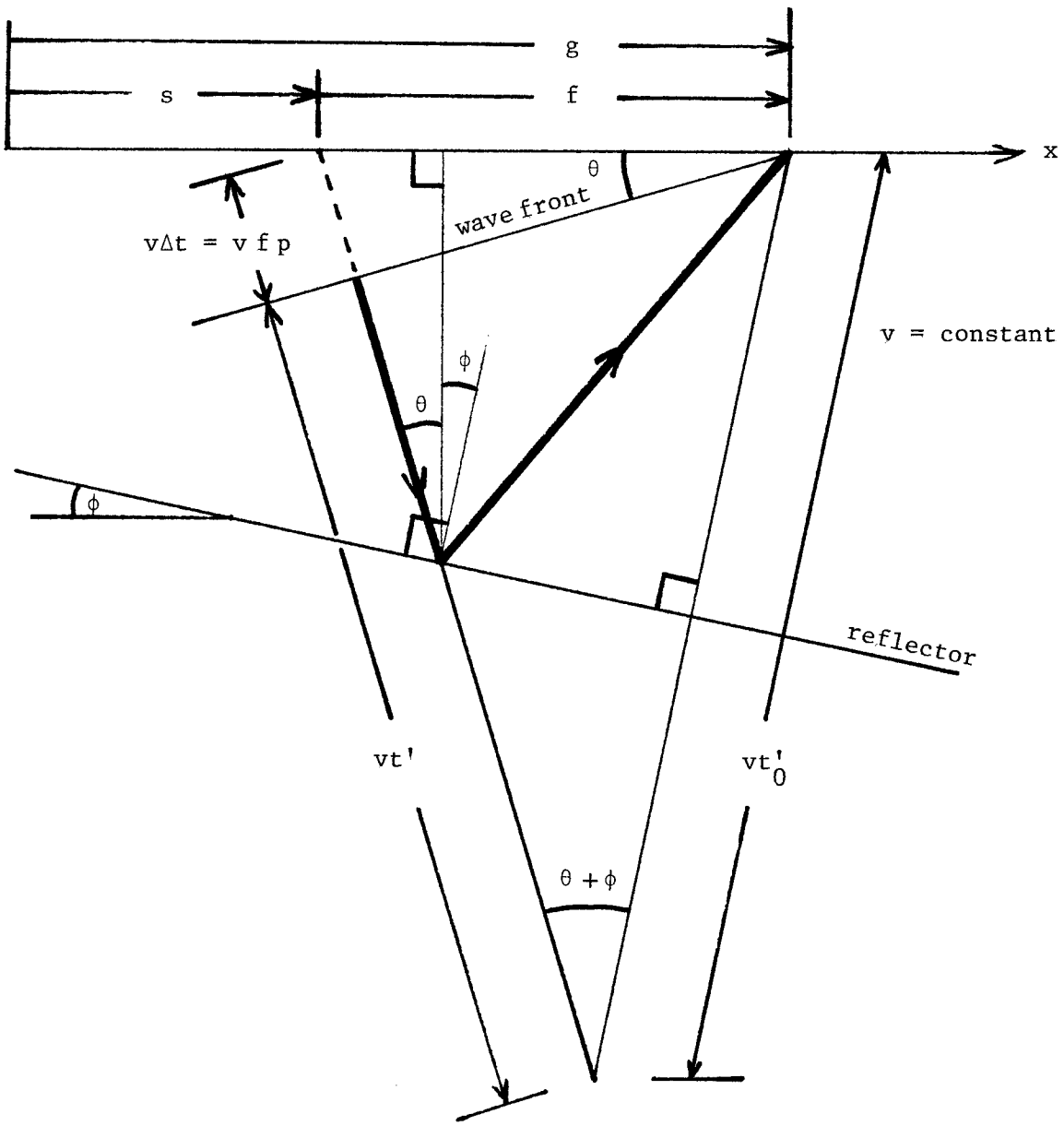

Figure 4.1. The ray path and coordinate definitions for a reflector of dip ϕ . Note that t'_0 is the zero-offset two-way travel time, but is no longer the $p = 0$ ray path. Compare with Figure 2.8. The relation

$$\frac{t'}{t'_0} = \cos(\theta+\phi)$$

is apparent in the figure for a constant velocity medium. Figure 4.3 shows the resultant p-gather for $\phi = 15$ degrees.

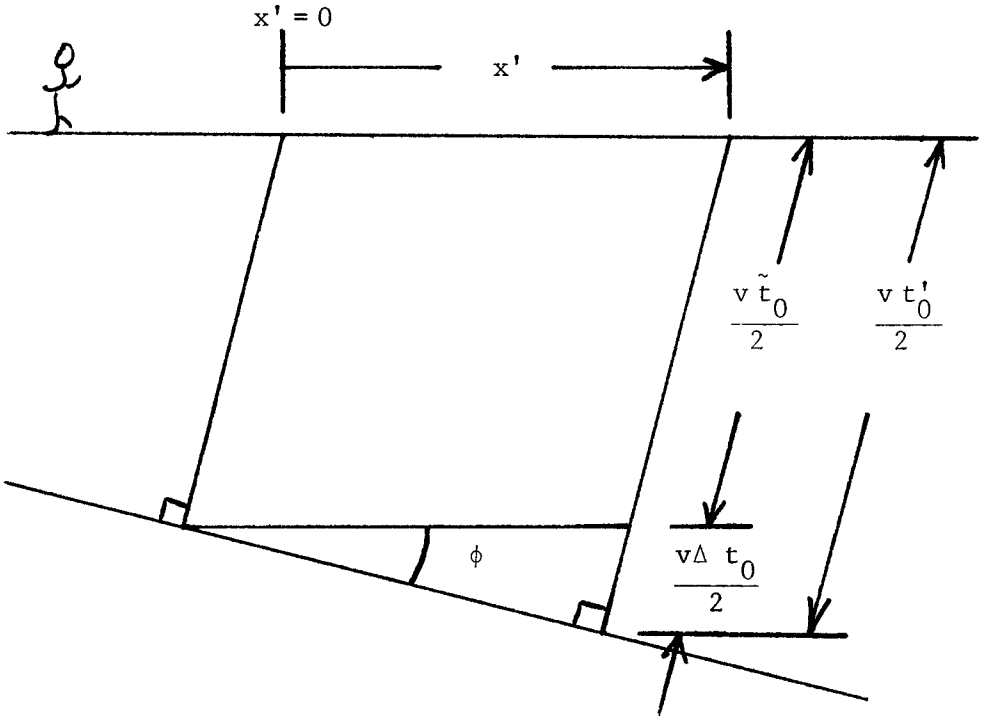

Figure 4.2. Diagram showing that the zero-offset travel time, t'_0, is a function of the horizontal coordinate x' when the reflector is dipping. When we define a zero for the x' coordinate, we can then define $\tilde{t}_0$ to be a property of the reflector. The relation

$$t'_0(x') = \tilde{t}_0 + \frac{2\,x'\,\sin\phi}{v} \tag{4.2}$$

can be written, making explicit the dependence of t'_0 on x'.

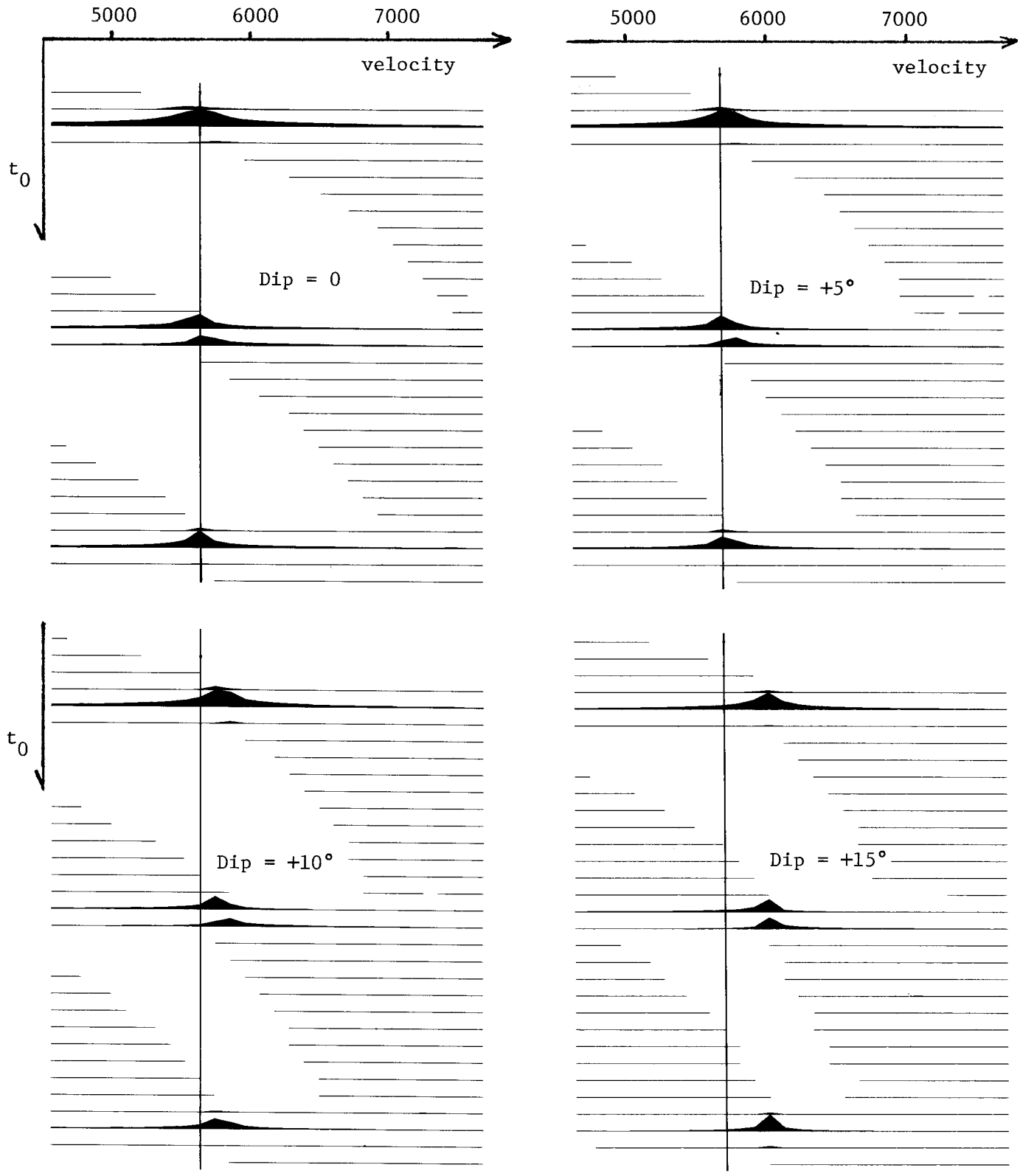

Figure 4.4. Continued on next page.

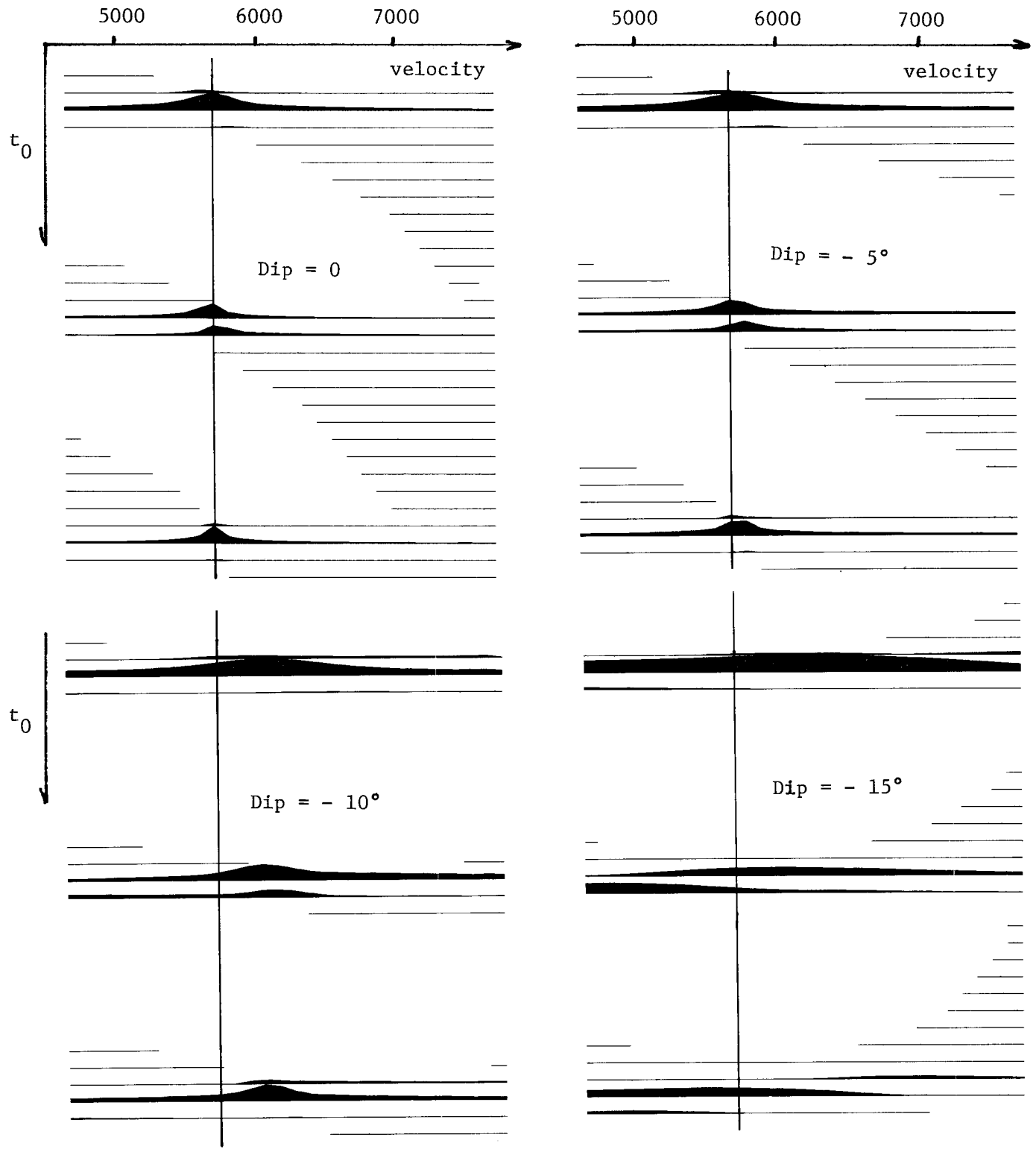

Figure 4.4. The effect of a dipping layer on velocity estimates done in slant frames using interpretation coordinates and only positive values of p. The velocity profiles are from synthetic data with three events, all dipping at the specified angle. The vertical line on each profile shows the "true" velocity: 5700 ft/sec.

no longer the $p=0$ travel time. Indeed, it is not even a property of only the reflector depth and velocity, but is a function also of the shot or geophone coordinate, x'. This functional dependence is described in Figure 4.2, where we have defined $\tilde{t}_0$ to be the value of t'_0 at $x'=0$. For an agreed upon origin for the x' coordinate, the quantity $\tilde{t}_0$ becomes a property of the reflector.

We combine equation (4.1) with equation (4.2) from Figure 4.2.

$$t'(p, x') = \left(\tilde{t}_0 + \frac{2x'\sin\phi}{v}\right)\cos(\theta+\phi) \qquad (4.3)$$

where we have now made explicit the dependence of the arrival time, t' on both p and x'.

Figure 4.3 shows a p-gather with $t'(p, x'=\text{const})$ for a dip angle $\phi=15°$. This is the gather which would result in a dipping environment with no attempt made to transform to interpretation coordinates. Equations (3.17) and the accompanying discussion in Chapter 3 describe the method by which we incorporate interpretation coordinates into velocity estimation.

Figure 4.4 shows the result of velocity estimation using interpretation coordinates in a dipping environment. Only positive values of p were used in the estimation simulating a one-sided spread. The results show that for the larger angles of dip, interpretation coordinates alone will not provide a sufficiently high order dip correction, and migration before velocity estimation appears to be the desirable alternative.

The Role of Migration

In this section we will show the effect of prior migration of slant frame data on a subsequent velocity analysis. For a review of migration, see for example, Peterson and Walter (1974). Migration will

be defined here simply as a process by which seismic data is converted to a reflectivity map.

Doherty (1975) has shown that when data is migrated prior to velocity analysis, reflectors of arbitrary curvature can be correctly treated in the manner of horizontal layers in the velocity estimation procedure. One must be careful, however, to insure that one is in a coordinate system whose gathers display a common subsurface reflection point in a flat layered earth. Such coordinate systems are CMP coordinates in the standard geometry and interpretation coordinates in the slant frames.

We shall describe the effect of migration first in the CMP geometry, and then draw a parallel for slant frames. Since migration corrects errors due to non-zero reflector dip, we investigate a reflector which contains all dips: a point scatterer.

Figure 4.5 shows a point scatterer at depth z_0 viewed with a single source and receiver separated by offset, f. The arrival time, t, for energy reflected from the scatterer is found by geometry to be

$$t = \frac{1}{v}\sqrt{h^2 + z_0^2} + \frac{1}{v}\sqrt{(f-h)^2 + z_0^2} \qquad (4.4)$$

This arrival time function will describe a pseudo-hyperbola when viewed in a common offset section (y,t). We used the parameter, h, in Figure 4.5 to simplify expression (4.4), but it can be converted to the midpoint coordinate, y, provided that f is held constant, by the simple transformation

$$h = y - y_0$$

with y_0 a constant.

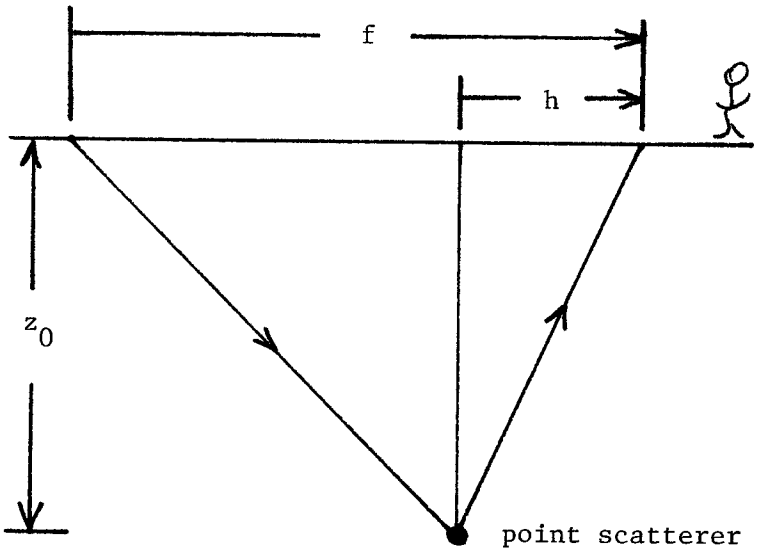

Figure 4.5. A ray path diagram for a point scatterer in CMP coordinates used to obtain equation (4.4).

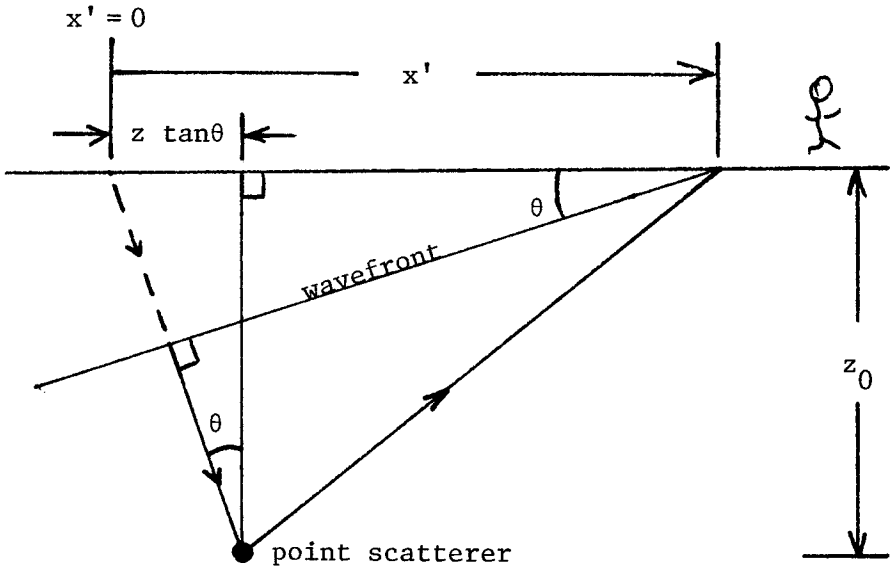

Figure 4.6. Ray path diagram for a point scatterer in slant frames used to obtain equation (4.7).

Now migration can be viewed as a process which will collapse the pseudo-hyperbolic arrival curve to the point at its apex. Let us locate the apex of the curve implied by (4.4). It must occur at such a value of h that

$$\left(\frac{\partial t}{\partial h}\right)_f = 0 \tag{4.5}$$

or, when

$$h = \frac{f}{2} \tag{4.6}$$

Notice that this configuration has the point scatterer reflecting as if it were a horizontally flat reflector, and that the process of migration forces this configuration to be the only one for which energy is present. As we would expect from this result, and as was shown by Doherty, velocity estimation done after migration using a theory for a horizontally layered earth will give accurate results even in a region of complex reflector topography.

Turning our attention to the arrival times for a point scatterer in slant frames, we view Figure 4.6. The geometry of the figure indicates that for a p-section (data in (x', t') coordinates for a constant p), the arrival times will be of the form,

$$t' = \frac{1}{v}\sqrt{(x' - z_0\tan\theta)^2 + z_0^2} + \frac{z_0}{v\cos\theta} - x'p \tag{4.7}$$

The above is an asymmetric pseudo-hyperbolic curve with its apex at x' such that

$$\left(\frac{\partial t'}{\partial x'}\right)_p = 0 \tag{4.8}$$

or, when

$$x' = 2 z_0 \tan\theta \qquad (4.9)$$

As in the case of the standard geometry, (4.9) indicates that the apex of the pseudo-hyperbolic curve occurs when the point scatterer reflects as if it were a horizontally flat reflector. We conclude from this result that migration as a pre-velocity analysis processor will have the same result in slant frames that Doherty showed it to have in the standard geometry: that a proper velocity estimation can then proceed assuming all reflectors to be horizontally flat. We must, however, choose CMP coordinates in the standard frame and interpretation coordinates in the slant frame.

Wave Equation Migration Coefficients

We now describe the coefficients necessary for data in slant frames to be migrated using the finite difference approach to the wave equation. (See Claerbout 1970, 1971, Claerbout and Doherty 1972, and Doherty, 1975.) The choice of wave equation migration for this discussion is not meant to imply that data in slant frames cannot be migrated using other schemes.

Let us at this time generalize the true subsurface velocity to be a function of both the vertical and horizontal coordinates. This quantity will be denoted $\tilde{v}(x,z)$. We also introduce a velocity $\bar{v}(z)$ which will be a velocity estimate, one that we specify as a function of depth. The velocity $\bar{v}$, is to be used as an input velocity for the migration. The equations which are developed in this section allow a migration of slant frame data to be done in a medium with velocity a function of both x and z .

An upcoming plane wave, $U(x, z, \tilde{t})$, in the earth with some propagation angle $\theta = \arcsin(pv)$ can be described by

$$U(x, z, \tilde{t}) = w(\tilde{t}) * \delta\left(\tilde{t} - \frac{x \sin\theta}{v} + \frac{z \cos\theta}{v}\right) \qquad (4.10)$$

where $w(\tilde{t})$ is the waveform and $\tilde{t}$ rather than t is used as the time coordinate since we have previously used t to be the shot-to-geophone time.

Equation (4.10) suggests the following coordinate transformation for anticipated use with the wave equation.

$$x' = x + \int_0^z \tan\theta(z)\, dz \qquad (4.11a)$$

$$z' = z \qquad (4.11b)$$

$$t' = \tilde{t} + \int_0^z \frac{dz\, \cos\theta(z)}{\bar{v}(z)} - x \frac{\sin\theta(z)}{\bar{v}(z)} \qquad (4.11c)$$

or expressing the angles in terms of the ray parameter, p,

$$x' = x + \int_0^z \frac{p\, \bar{v}(z)\, dz}{(1-p^2\bar{v}^2(z))^{1/2}} \qquad (4.12a)$$

$$z' = z \qquad (4.12b)$$

$$t' = \tilde{t} + \int_0^z \frac{(1-p^2\bar{v}^2(z))^{1/2}}{\bar{v}(z)}\, dz - x\,p \qquad (4.12c)$$

where the primed variables represent the coordinates of choice for the migration. The coordinates x and z are earth-based, and equation (4.12a) describes the interpretation coordinate transformation. The variable, x', therefore, represents the same quantity which it did in previous sections, the horizontal coordinate of the slant stacked data.

Likewise we notice that the coordinates $\tilde{t}$ and t' have the usual relationship at $z = 0$. The generalization to depth dependence implies that we now prepare to downward continue the surface data to depth.

The transformation equations (4.12) define a new downgoing wave field with the relation

$$U(x, z, \tilde{t}) = U'(x', z', t') \tag{4.13}$$

to be the wave field.

We wish to describe the wave equation

$$U_{xx} + U_{zz} = \frac{1}{\tilde{v}(x,z)} U_{\tilde{t}\tilde{t}} \tag{4.14}$$

in the primed coordinates, so we compute the proper derivatives.

$$U_x = U'_{x'} - p\, U'_{t'}$$

$$U_{\tilde{t}} = U'_{t'}$$

$$U_z = U'_{x'} \left(\frac{p\bar{v}}{(1-p^2\bar{v}^2)^{1/2}}\right) + U'_{z'} + U'_{t'} \left(\frac{(1-p^2\bar{v}^2)^{1/2}}{\bar{v}}\right)$$

and

$$U_{xx} = U'_{x'x'} - 2\,p\,U'_{x't'} + p^2\,U'_{t't'}$$

$$U_{\tilde{t}\tilde{t}} = U'_{t't'}$$

$$U_{zz} = \frac{p^2\bar{v}^2}{(1-p^2\bar{v}^2)} U'_{x'x'} + U'_{z'z'} + \frac{(1-p^2\bar{v}^2)}{\bar{v}^2} U'_{t't'}$$

$$+ \frac{2\,p\,\bar{v}}{(1-p^2\bar{v}^2)^{1/2}} U'_{x'z'} + 2\,\frac{(1-p^2\bar{v}^2)^{1/2}}{\bar{v}} U'_{z't'} + 2\,p\,U'_{x't'}$$

$$+ \left[\frac{\partial}{\partial z} \frac{p\bar{v}}{(1-p^2\bar{v}^2)^{1/2}}\right] U'_{x'} + \left[\frac{\partial}{\partial z} \frac{(1-p^2\bar{v}^2)^{1/2}}{\bar{v}}\right] U'_{t'}$$

Now substitution into the wave equation gives

$$U'_{x'x'} - 2\,p\,U'_{x't'} + p^2\,U'_{t't'} + \frac{p^2\bar{v}^2}{(1-p^2\bar{v}^2)^{1/2}}\,U'_{x'x'}$$

$$+ U'_{z'z'} + \frac{(1-p^2\bar{v}^2)}{\bar{v}^2}\,U'_{t't'} + \frac{2\,p\,\bar{v}}{(1-p^2\bar{v}^2)^{1/2}}\,U'_{x'z'}$$

$$+ \frac{2(1-p^2\bar{v}^2)^{1/2}}{\bar{v}}\,U'_{z't'} + 2\,p\,U'_{x't'} + \left[\frac{\partial}{\partial z}\,\frac{p\,\bar{v}}{(1-p^2\bar{v}^2)^{1/2}}\right]U'_{x'}$$

$$+ \left[\frac{\partial}{\partial z}\,\frac{(1-p^2\bar{v}^2)^{1/2}}{\bar{v}}\right]U'_{t'} = \frac{1}{\tilde{v}^2}\,U'_{t't'} \qquad (4.15)$$

We now drop the $U'_{z'z'}$ as we make the Fresnel approximation and notice that the $U'_{x't'}$ terms add to zero. In addition, we drop the $U'_{x'z'}$ term because it has been shown to be small in previous work (see, for example, Doherty, 1975). This term may be retained however, if a higher order approximation to the differential equation is desirable.

Collecting all remaining terms gives

$$U'_{z't'} = \frac{\bar{v}(z)}{2}\,(1 - p^2\bar{v}^2(z))^{-3/2}\,U'_{x'x'}$$

$$+ \frac{\bar{v}(z)}{2(1-p^2\bar{v}^2(z))^{1/2}}\left(\frac{1}{\bar{v}^2(z)} - \frac{1}{\tilde{v}^2(x,z)}\right)U'_{t't'}$$

$$- \frac{p\bar{v}(z)\,\bar{v}_z(z)}{2(1-p^2\bar{v}^2(z))^2}\,U'_{x'} - \left[\frac{p^2\bar{v}\,(z)\,\bar{v}_z(z)}{2(1-p^2\bar{v}^2(z))} + \frac{\bar{v}_z(z)}{2\bar{v}(z)}\right]U'_{t'}, \qquad (4.16)$$

The first term on the right hand side is the new form of the diffraction term. The second term allows us to correct for propagation through regions of lateral inhomogeneity (provided we know the form of $\tilde{v}$). These two terms have been treated in detail in previous papers, but the final two terms involving $\bar{v}_z$, are unique to the stratified media transformation.

We now look at these two terms,

$$U'_{z't'} = - \frac{p\bar{v}(z)\bar{v}_z(z)}{2(1-p^2\bar{v}^2(z))^2} U'_{x'} - \left[\frac{p^2\bar{v}(z)\bar{v}_z(z)}{2(1-p^2\bar{v}^2(z))} + \frac{\bar{v}_z(z)}{2\bar{v}(z)} \right] U'_{t'}$$

and separate the operations

$$U'_{z't'} = - \frac{p\bar{v}(z)\bar{v}_z(z)}{2(1-p^2\bar{v}^2(z))^2} U'_{x'} \qquad (4.17a)$$

$$U'_{z't'} = - \left[\frac{p^2\bar{v}(z)\bar{v}_z(z)}{2(1-p^2\bar{v}^2(z))} + \frac{\bar{v}_z(z)}{2\bar{v}(z)} \right] U'_{t'} \qquad (4.17b)$$

To equation (4.17a) let us transform out the t and x dependence, and to equation (4.17b) let us integrate with respect to t . Then, recombining the equations we have

$$U'_{z'} = - \left\{ \frac{p\bar{v}_z(z)}{2(1-p^2\bar{v}^2)^2} \left(\frac{\bar{v}(z)k_{x'}}{\omega} \right) + \frac{p^2\bar{v}(z)\bar{v}_z(z)}{2(1-p^2\bar{v}^2(z))} + \frac{\bar{v}_z(z)}{2\bar{v}(z)} \right\} U' \qquad (4.18)$$

To determine the function of this combined term, we look at the last term in the coefficient. This takes the form,

$$U_z = - \frac{\bar{v}_z(z)}{2\bar{v}(z)} U$$

which has solutions

$$U(z) = U(z+\Delta z) \left[\frac{\bar{v}(z+\Delta z)}{\bar{v}(z)} \right]^{1/2}$$

and is clearly an amplitude correction for transmission across a region of velocity gradient.

Without permuting terms, we rewrite equation (4.18) in the form,

$$U'_{z'} = \left[a_3\left(z, p, \frac{\bar{v}k_{x'}}{\omega}\right) + a_2(z,p) + a_1(z) \right] U' \qquad (4.19)$$

The factor a_1 is a function only of z and will be non-zero for even the simplest case, being vertical incidence ($p = \theta = 0$) of a plane wave front onto an interface. This is shown in Figure 4.7a.

The factor a_2 is a function of both z and p, and will be non-zero only for $p \neq 0$. Figure 4.7b shows the simplest case of a non-zero a_2 : a plane wave front incident on an interface at an angle given by the slant frame transformation (i.e., θ) .

The factor a_3 is a function of z, p, and $k_{x'}$. In addition to a sensitivity to z and p, as with a_2, it is also sensitive to a non-zero $k_{x'}$ (i.e., a non-zero $\partial/\partial_{x'}$). The incident wave front of Figure 4.7b follows a curve x' = constant, so that $\partial/\partial_{x'} = k_{x'} = 0$ for this case. The factor a_3 is therefore sensitive to deviations from the ideal incident angle, θ. Figure 4.7c shows a simple case of a distorted (i.e., non-planar) wave front impinging on an interface for which case a_3 is non-zero.

At this point a disclaimer should be made in regard to the interpretation of $(a_1 + a_2 + a_3)$ in equation (4.19) as a transmission coefficient. It will be true only to the extent that the gradients of density are everywhere zero; any non-zero density gradient will change the form of equation (4.18). However, we will not reformulate the problem to include the density because we do not foresee any advantages to including the transmission terms (equation (4.18)) in our difference formulation of the transformed wave equation (4.16). These terms may be considered amplitude correction terms, and although they may be interesting in some modeling cases (for example, modeling the dim regions below bright spots), they will be ignored for our applications.

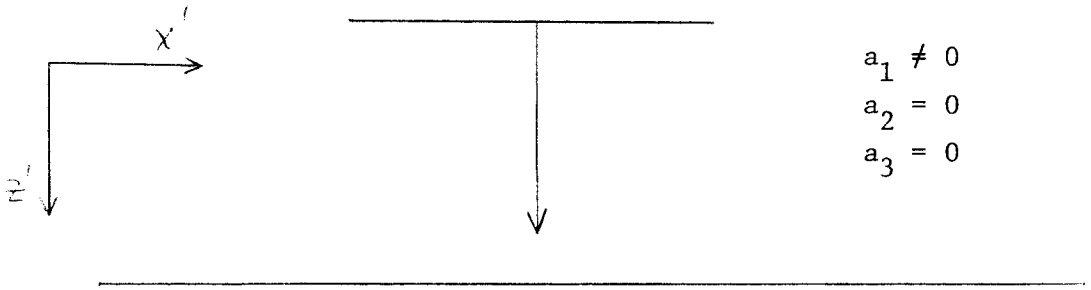

Fig. 4.7a. The simplest case of vertical plane wave incidence ($\theta = p = 0$) for which all but a_1 is zero in equation (4.28).

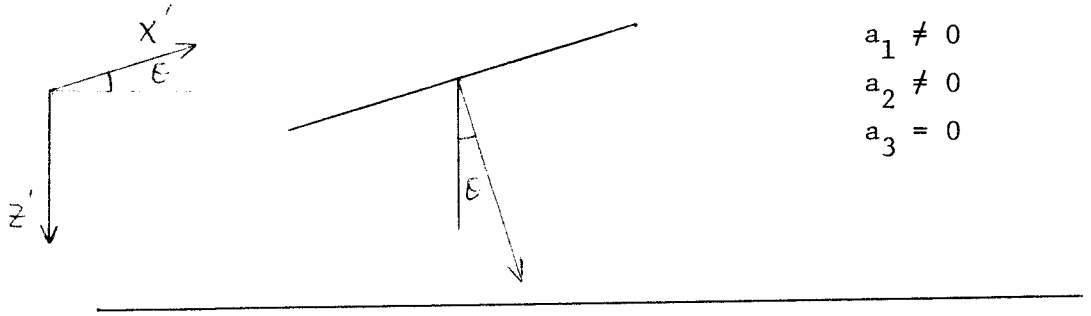

Fig. 4.7b. Plane wave incidence at the coordinate transformation angle θ for which both a_1 and a_2 are non-zero in equation (4.28).

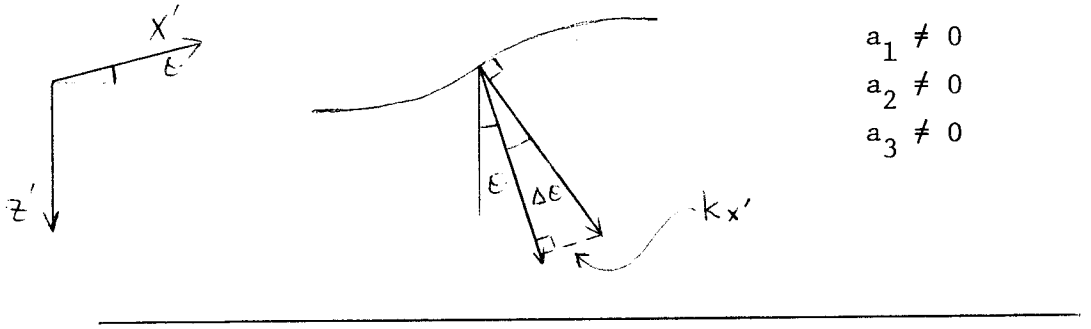

Fig. 4.7c. Non-plane wave incidence at the approximate coordinate transformation angle θ showing a simple situation where k_x, (or equivalently, D'_x,) is non-zero, causing a_3 , along with a_1 and a_2 , to be non-zero. The factor a_3 is therefore sensitive to deviations from the transformation angle θ .

Dropping these transmission terms leaves us an equation of the form

$$U'_{z't'} = \frac{\bar{v}(z)}{2} \left(1 - p^2\bar{v}^2(z) \right)^{-3/2} U'_{x'x'} + \frac{\bar{v}(z)}{2(1-p^2\bar{v}^2(z))^{1/2}} \left[\frac{1}{\bar{v}^2(z)} - \frac{1}{\tilde{v}^2(x,z)} \right] U'_{t't'} \tag{4.20}$$

showing that we may apply standard wave equation techniques to the migration of slant frame data in a depth dependent velocity medium.

Strong Lateral Velocity Inhomogeneity

Migration of data in regions where the acoustic velocity is only a function of depth need only concern itself with wave propagation effects on the upcoming wave. This is true even when reflectors have arbitrary structure, and is due to the fact that the downgoing wave is subject only to transmission effects.

When the subsurface velocity becomes strongly laterally variable to the point that the downgoing wave becomes multibranched, then a complete migration picture must explicitly consider both the upcoming and downgoing waves.

An equation like (4. 20) can be used directly on the upcoming wave to downward continue it to depth through any complicated velocity medium, but this process will reveal true reflector structure only if the downgoing wave was a true plane wave when it was incident on the reflectors. The slant stack process which we have been discussing creates plane waves at the surface, and they may or may not remain so at depth.

Figure 4.8 shows an example of severe sea floor topography which will distort a downgoing wave front because of the severe lateral velocity variation. We begin by defining a "datum plane wave" at some depth z_1, below the sea floor on a mesh in a computer. Then using an equation like (4.20), project this wave back up to the surface z_0 going through the severe lateral velocity variations.

The resulting wave field at z_0 will be the downgoing wave, $D(z_0, s, t)$, that we will wish to synthesize at the surface by a generalized slant wave stack. We must do a wave stack of the surface gathers so that each shot is "fired" in the proper sequence and with the proper amplitude so that the desired downgoing wave field, $D(z_0, s, t)$, is created just below the surface.

In the notation of equation (2.7), the trace $P'(g_0, t')$ resulting from the wave stack on a gather to produce downgoing wave $D(z_0, s, t)$ is given by

$$P'(g_0, t') = \sum_{s,\tau} D(z_0, s, t'-\tau)\ P(g_0, s, \tau) \qquad (4.21)$$

where $P(g_0, s, t)$ is the common geophone gather at g_0. Equation (4.21) defines the generalized wave stack.

When the wave stack (4.21) is done on the surface data, equations like (4.20) can then be used to downward continue the upcoming wave to the reflectors, since we know they have been illuminated by a plane wave front. The combination wave stack described in (4.21) followed by wave equation migration using an equation similar to (4.20) constitutes a complete and proper migration.

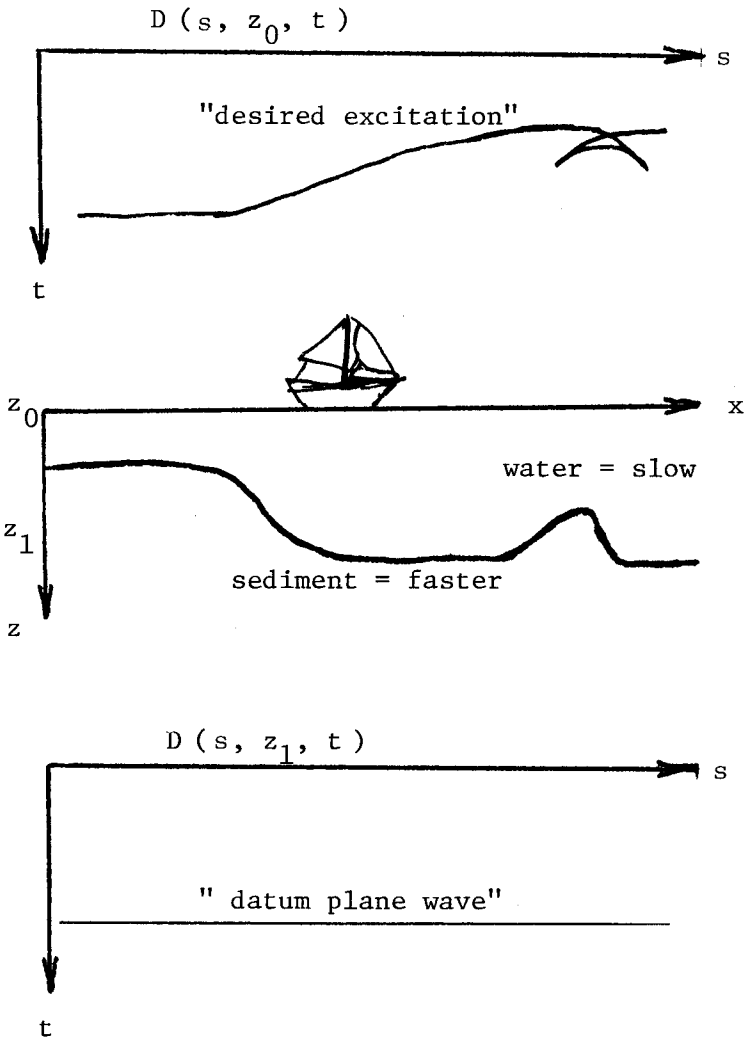

Figure 4.8. In order to achieve a downgoing plane wave at the datum depth z_1, another wave "desired excitation" must be initiated at z_0. The "desired excitation" may be computed by projecting the "datum plane wave" up through the sea floor topography.

Doherty's (1975) result showed that migration with an approximate velocity prior to a complete velocity estimate will render the estimation structure independent. The method of this section, which involves migration of both the upcoming and downgoing wave permits prior migration to become a more generalized procedure. Any information on strong lateral velocity variations can now be included in the pre-velocity analysis migration to thereby reduce its distorting effect on velocity estimation. Severe sea floor topography is the most likely situation in which the above procedure may be desirable.